Pergamon

Scripta Metallurgica et Materialia, Vol. 31, No. 6, pp. 713-718, 1994

0956-716X/94 $6.00 + 00

# Laser Surface Alloying of Aluminum on Copper Substrate

I. Manna[•], S. Abraham[•], G. Reddy[•], D.N. Bose[+], T.B. Ghosh[#] and S.K. Pabi[•]
[•]Metallurgical Engg. Dept., [+]Mater. Sci. Center, [#]Physics Dept.
*Indian Institute of Technology, Kharagpur 721 302, W.B., INDIA*

(Received March 23, 1994)
(Revised May 11, 1994)

## Introduction

Laser surface alloying (LSA) involves melting of a surface-deposit with a part of the underlying substrate by the directed energy laser beam to form an alloyed zone (AZ), confined to a very shallow depth from the surface [1-3]. Lasing is carried out either in the continuous wave (CW) or pulsed mode of irradiation. CW lasers with a suitable sweeping facility allows larger surface-area coverage and a deeper melt-depth penetration. On the other hand, pulsed mode of lasing is more suited to achieve higher heating/cooling rates, and convenient monitoring of the successive stages of microstructural and/or compositional modulation during laser aided surface treatment. In practice, pulsed laser treatment enables a very high density of directed energy of 0.1 to 10 $J/mm^2$ being delivered in short pulses of $10^{-3}$ to $10^{-12}$s to achieve an extreme heating/cooling rate of $10^6$-$10^{13}$ K/s, a thermal gradient of $10^8$-$10^{10}$ K/m, and a solidification velocity of 1-30 m/s in less than 10 μm from the surface [1-5]. This leads to the formation of novel microstructures including extended (metastable) solid solution and even, an amorphous state, through melting, intermixing, and rapid diffusion within an extremely short period of time. The present study concerns LSA of Al coated on Cu, with a pulsed ruby laser to investigate the microstructural evolution and compositional changes in the AZ as a function of the number of pulses. Finally, an attempt has been made to calculate the heating/cooling rates, and depth of melting accomplished during laser irradiation in this study, by determining a one-dimensional temperature profile in the AZ as a function of time and depth, respectively.

## Experimental

About 10 mm square and 3 mm thick flat pieces were cut from rolled and annealed sheets of pure Cu. The samples were mechanically polished with diamond dust, followed by chemical cleaning with acetone, prior to coating with 0.2 μm thick Al by physical vapour deposition. The coated samples were subjected to ruby laser (wavelength, $\lambda$ = 0.694 μm) irradiation in air for varying number of 30 ns pulses with a 0.2 $J/mm^2$ energy density. Laser parameters like beam diameter, energy density, pulse duration, and source-specimen distance were standardized by a number of preliminary trials to optimize the LSA condition for the present set of samples. A detailed investigation on microstructural evolution in course of lasing with increasing number of laser pulses was carried out using a scanning electron microscope

(SEM) in the secondary electron mode. The extent of surface alloying and related information about surface chemistry were studied by X-ray photoelectron spectroscopy (XPS) with a VG ESCA Lab MK II spectrometer using Mg-Kα (1253.6 eV) radiation, operating at 12 kV, 10 mA. The possible presence of a thin oxide film on the surface was removed by sputtering with $Ar^+$ ions before recording the XPS spectrum. The binding energy of the carbon 1*s* peak was taken as the energy reference.

## Results and Discussion

### *Studies on surface microstructure*

Each laser pulse induces a transient melting followed by a rapid solidification, resulting into a progressive microstructural refinement with an increasing number of pulses on the same spot. Apparently, the depth of melting under the present experimental condition (~8000Å) covers the deposit and part of the underlying substrate, which will be confirmed by mathematical modelling of the temperature profile in the AZ, at an appropriate section of this report. Figure 1 reveals a typical uniform and cellular microstructure following four laser pulses. The degree of microstructural refinement and homogeneity appears to reach a limiting stage between six to eight pulses. Figure 2 shows the periphery of a laser treated zone following five pulses on the same spot. The difference in microstructure between the centre (Fig.1) and periphery (Fig.2) of the laser irradiated region arises because of the absence of a relative motion between the sample and beam. A careful examination of a large number of microstructures reveals the presence of some surface porosity, especially in the early stages of pulse treatment (Figs.1 and 2). Furthermore, microstructural evidences suggest that solidification may proceed in successive 'wave-like' stages leaving behind a series of surface ripples (Fig. 3). A similar alternate sequence of bright (microsegregation free) and dark (dendritic/eutectic) regions in the microstructure of laser induced rapid solidification in eutectic/hypo-eutectic Al-Cu alloys have earlier been termed as a 'banded structure' [6]. We would like to point out that a considerable solute (*i.e.* Ta) segregation along the edges of the melt puddles has previously been evidenced in a study on the LSA of the Ni-Ta system with a CW-$CO_2$ laser [7]. Furthermore, a number of particulate phases, either equilibrium or metastable intermetallics (shown by arrowhead in Fig. 4), appear in the microstructure with an increase in the number of pulses. A detailed XPS study was undertaken to investigate the surface chemistry and identity of these particles.

### *Studies on surface chemistry*

Figure 5 shows the Cu 2*p* photoelectron peak of a sample exposed to six laser pulses of a 30 ns duration with an incident energy density of 0.2 $J/mm^2$. The absence of peak-asymmetry or shake-up satellite appears to indicate that the Cu(II) phase was not present. Figure 6 displays a typical X-ray excited $CuL_3VV$ peak from the same sample. Both sharpness of the $CuL_3VV$ peak in Fig. 6, and relatively small inherent width or full width at half-maximum (FWHM = 1.46 eV) of the Cu 2*p* peak in Fig. 5, seem to suggest that the Cu(I) phase was also absent. The sum of the binding energy of the photoelectron, and kinetic energy of the Auger electron, referred to as the Auger parameter, has been calculated to be 1851.2 ± 0.6 eV for the present sample [8]. According to the existing data in the literature [8], the calculated Auger parameter may be attributed to either pure Cu or an intermetallic phase like $Al_2Cu$, AlCu, etc. [9]. Figure 7 reveals the Al 2*p* photoelectron peak obtained from the sample exposed to seven pulses. The high binding energy tail may be attributed to the superimposed Cu 3*p* peak at 78.8 eV. Assuming a gaussian distribution of intensity as a function of binding energy about the anticipated peak positions stated in the literature [8], the broad Al 2*p* peak has been resolved into the respective constituent components in Fig. 7 (shown by arrowhead). According to the best fit profile, the peaks of the resolved components are located at 74.2 and 75.5 eV with corresponding FWHM values of 1.7 and 2.1 eV, respectively (Fig. 7). Thus, it appears that Al is present in two different chemical states in the Cu matrix. Comparing with the relevant data in the literature [8], the peak at 75.5 eV may be attributed to $Al_2O_3$. Thin film of $Al_2O_3$ on the sample surface is expected to be present because the lasing operation was carried out in air. The other peak, at 74.2 eV, is believed to be due to metallic Al. However, the 2p peak for pure Al is ideally located at 72.92 eV [8]. Formation of Al(II) intermetallic phases may lead to shifting of the Al 2*p* peak position to a binding energy value higher than that for pure Al. The ratio between the area under a given peak and the respective sensitivity factor (obtained from the literature [8]) may be assumed to be proportional to the atomic fraction of the element concerned [10]. The ratio between the atomic fractions of Cu to that of Al in the laser alloyed surface, as determined from the respective areas under the curves of Cu 2*p* and Al 2*p* (74.2 eV), is 0.51 with an uncertainty limit of ± 0.05 (due to a possible error in selecting the background intensity and/or using the sensitivity factor values from the literature). Thus, the stoichiometry of the intermetallic compound appears to be $Al_2Cu$. Presence of an equilibrium $Al_2Cu$ or $\theta$ phase is indirect proof for the formation of a Cu rich solid solution of Al in Cu, according to the Cu-Al phase diagram [9]. However, the presence of additional intermetallic phases like AlCu cannot be ruled out, because of the close proximity of the corresponding peaks and lack of precise peak position data in the literature. Available data in the literature on Al 2*p* photoelectron peak indicate that the FWHM is about 1.8 eV [8]. The observed higher value of FWHM (2.1 eV, cf Fig.6) for the peak at 75.5 eV appears to suggest that Al may exist in the matrix in more than one metastable state. It is known that a number of metastable phases appear in the microstructure in Al-Cu system before the equilibrium $Al_2Cu$ phase may form [8]. Furthermore, the extreme heating/cooling rates in pulsed laser treatments may result into the formation of extended solid solution or metastable phases [1,2]. Since the XPS data represent the chemistry of a typically less than 4 nm thick surface layer, it is reasonable to conclude that the few top atomic layers of the laser treated samples in the present study consist of different chemical states of Cu-Al phases including $Al_2Cu$ and a thin $Al_2O_3$ film, but no $Cu_2O$ or CuO. Absence of $Cu_2O$ or CuO is expected as any oxide of Cu will be thermodynamically unstable in the presence of Al at all temperatures.

*Determination of temperature profile by numerical calculation*

The field equation for heat transfer during laser irradiation of solids in pulses assuming a one-dimensional heat flow condition (as the laser beam diameter is much larger compared to the thermal diffusion length [4,11]) may be written as follows :

$$\rho C_p \frac{\partial T(z,t)}{\partial t} = \alpha\ I_o(t)\ (1-R)\ \exp\ (-\alpha z) + \frac{\partial}{\partial z}\ [K\ \frac{\partial T(z,t)}{\partial z}]$$

where, $\rho$ = density, $C_p$ = specific heat, T = absolute temperature, z = vertical depth from the surface parallel to the beam, t = time, $\alpha$ = absorption coefficient, $I_o$ = incident laser beam intensity, R = reflectivity, and K = thermal conductivity. It may be noted that the discontinuous changes of the laser coupling parameters ($\alpha$ and R) and materials parameters (K, $C_p$, $\rho$) with the solid to liquid phase transition render the analytical solution of this heat balance equation impossible. In the present study, this equation has been solved numerically using the explicit finite difference method by : (i) considering a triangular wave function (as an approximation to the actual near-gaussian distribution) of $I_o$ instead of the usual practice of assuming a mode locked square wave function, (ii) using the convergence condition of $K[\Delta t/[C_p\rho(\Delta z)^2] < 0.5$ with the boundary conditions of T = 300K at t = 0 at any z, and T = 300K at all t for z > 20 μm, and (iii) obtaining the appropriate values of the coupling and materials parameters from the literature [14,15].

Figure 8 presents the predicted temperature profile as a function of time at different depths from the surface. The changes in curvature (shown by arrowhead) at 933K for the profile at z = 0.0 μm (surface), and at 1357K for the profile at z = 0.5 μm, correspond to the melting temperatures, and hence, the solid-liquid phase transition of Al and Cu, respectively. It is interesting to note that the peak temperature ($T_{max}$) in the present study is attained at $t<t_p$ (where, $t_p$ = pulse duration) due to the triangular wave function of $I_o$, in contrast to $T = T_{max}$ at $t = t_p$ for the square wave function of $I_o$ [11]. In general, the temperature profile in this study (Fig. 8) appears similar to the earlier predictions for pure substrates [4,11-13].

Figure 9 illustrates the temperature profile as a function of z at t = 10, 15, 25 and 30 ns. In accordance with the T-t profile (Fig.8), the highest temperature distribution is attained at t (= 25 ns) < $t_p$ (= 30 ns). The intersection of the profiles for t = 15 and 30 ns in Fig.9 may once again be attributed to the triangular (instead of square) wave function of the input beam intensity. Figure 9 also confirms that temperature drops to below the melting point of Cu or Cu(Al) within a typical depth of 0.8 μm signifying that the LSA is confined to a very narrow depth (< 1 μm) from the surface. Finally, the heating and cooling rates computed from the present model are $1.5 \times 10^{11}$ and $3 \times 10^{10}$ K/s, respectively.

## Summary and Conclusion

The present study indicates that pulsed laser irradiation of Al coated Cu samples results into a progressive microstructural refinement, which reaches a limiting level at about six to eight laser pulses. The early stages of laser irradiation lead to the formation of a certain amount of surface porosity, which however, decreases with the progressive intermixing achieved through an increasing number of pulses. A detailed XPS analysis has revealed the presence of equilibrium precipitates like $Al_2Cu$, in addition to the formation of solid solution of Al in Cu. Finally, the modified mathematical model proposed is able to consider the melting and solidification in both the deposit and part of the underlying substrate, and predict a realistic temperature profile in the AZ. The cooling rate, as estimated from the present model, is orders of magnitude faster than that achievable in any rapid solidification technique developed to date.

## Acknowledgement

One of the authors (I.M.) gratefully acknowledges the partial financial support for this work from the *Indian National Science Academy*, New Delhi.

## Reference

[1] C. W. Draper and J. M. Poate, Internat.Met.Rev. **30**, 2 (1985).
[2] P. A. Molian, in: Surface Modification Technologies - An Engineer's Guide, T. S. Sudarshan (Ed.), Marcel Dekker Inc., New York 1989 (p.421).
[3] B. L. Mordike, in: Materials Science and Technology (vol.15), R. W. Cahn, P. Haasen, E. J. Kramer (Eds.), VCH, Weinheim, FRG 1991 (p.111).
[4] C. W. White and M. J. Aziz, in: Surface Alloying by Ion, Electron and Laser Beams, L. E. Rehn and S. T. Picraux (Eds.), A.S.M., Metals Park, Ohio, USA 1987 (p.19).
[5] M. v. Allem, in: Laser and Electron Beam Processing of Materials, C. W. White and P. S. Peercy (Eds.), Academic Press, London 1980 (p.6).

[6] M. Zimmermann, M. Carrerd, M. Gremand and W. Kurz, Mater.Sci.Engg. **A134**, 1278 (1991).
[7] C. W. Draper, J. M. Gibson, D. C. Jacobson, J. M. Poate, S. M. Shin and R. M. Rigsbee, J. Mater.Sci. **20**, 2303 (1985).
[8] M. P. Seah, in: Practical Surface Analysis by Auger and X-Ray Photoelectron Spectroscopy, D. Briggs and M. P. Seah (Eds.), Wiley, New York 1988 (p.477, 496, 511).
[9] T. B. Massalski (Ed.), Binary Alloy Phase Diagrams, (vol.1), A.S.M., Metals Park, Ohio 1986 (p.19).
[10] T. B. Ghosh and M. Sreemany, Appl.Surf.Sci. **64**, 59 (1993).
[11] P. Baeri, S. U. Campisano, G. Foti and E. Rimini, J.Appl.Phys. **50**, 788 (1975).
[12] R. F. Wood and G. E. Giles, Phys.Rev. **B23**, 2923 (1981).
[13] W. R. Wampler, D. M. Follstaedt and P. S. Peercy, in: Laser and Electron Beam Solid Interactions and Materials Processing, J. F. Gibbons, L. D. Hess and T. W. Sigmon (Eds.), North Holland, New York 1981 (p.567).

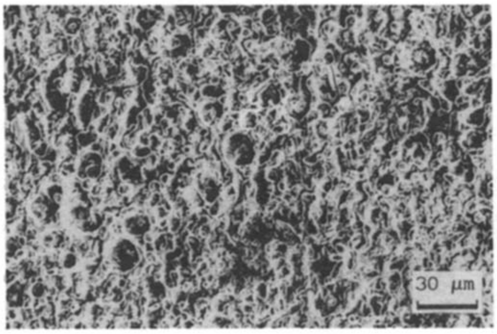


Fig.1: A uniform and fine cellular microstructure developed following four laser pulses on the same spot.

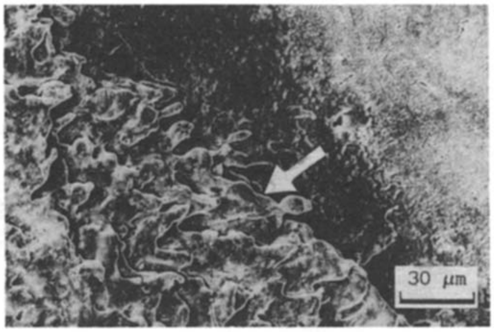


Fig.2: An interface (arrow-marked) between the unirradiated and laser-irradiated spot after five pulses.

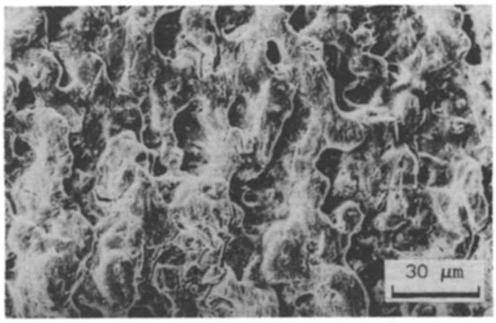


Fig.3: Surface ripples ('wave-like' features) developed in the microstructure after six laser pulses.

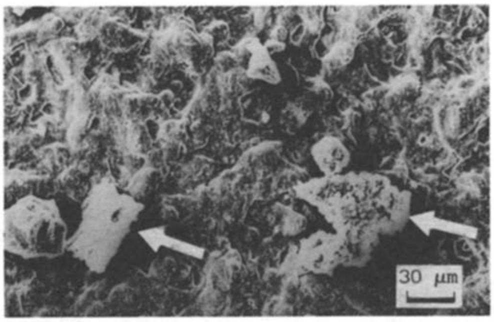


Fig.4: Particulate phases (shown by arrowhead) appearing in the microstructure after eight laser pulses.

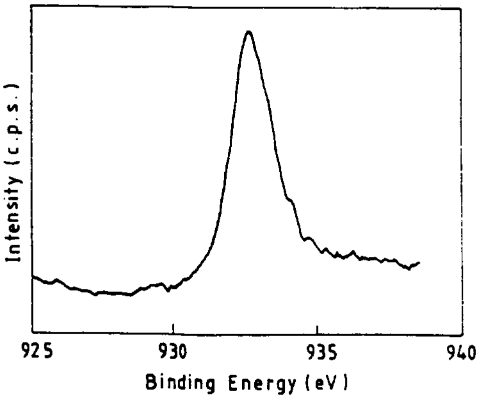


▲ Fig.5: Cu-2p photoelectron peak recorded at 1K with a time constant of 3.3 s.

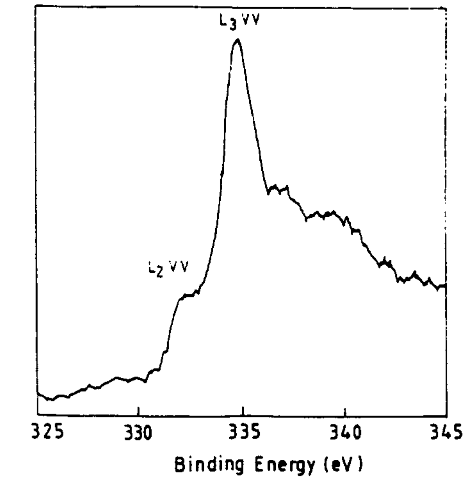


▲ Fig.6: X-ray excited Cu-L3 VV line recorded at 3×3K with a time constant of 3.3 s.

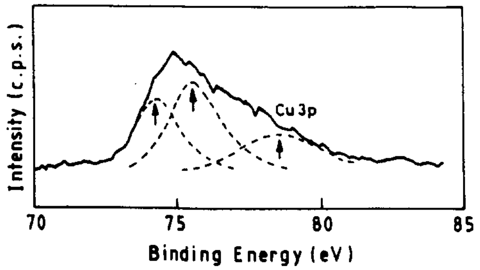


◀ Fig.7: Al-2p photoelectron peak recorded at 1K with a time constant of 3.3s. Arrowheads indicate the superimposed component peaks (see text).

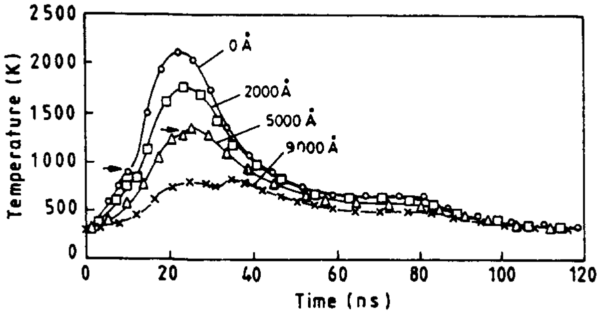


◀ Fig.8: Temperature profile as a function of time during laser irradiation. The arrow heads indicate melting of pure Al and Cu, respectively.

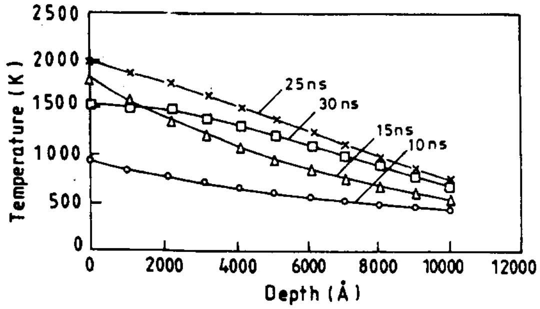


◀ Fig.9: Temperature profile as a function of depth from the surface at different stages of time within the laser irradiation pulse.